

This work was written as part of one of the author's official duties as an Employee of the United States Government and is therefore a work of the United States Government. In accordance with 17 U.S.C. 105, no copyright protection is available for such works under U.S. Law.

Public Domain Mark 1.0

<https://creativecommons.org/publicdomain/mark/1.0/>

Access to this work was provided by the University of Maryland, Baltimore County (UMBC) ScholarWorks@UMBC digital repository on the Maryland Shared Open Access (MD-SOAR) platform.

Please provide feedback

Please support the ScholarWorks@UMBC repository by emailing scholarworks-group@umbc.edu and telling us what having access to this work means to you and why it's important to you. Thank you.

A new technique for retrieval of tropospheric and stratospheric ozone profiles using sky radiance measurements at multiple view angles: Application to a Brewer spectrometer

Maria Tzortziou,^{1,2} Nickolay A. Krotkov,^{2,3} Alexander Cede,^{1,2} Jay R. Herman,² and Alexander Vasilkov⁴

Received 22 June 2007; revised 29 October 2007; accepted 26 December 2007; published 27 March 2008.

[1] This paper describes and applies a new technique for retrieving diurnal variability in tropospheric ozone vertical distribution using ground-based measurements of ultraviolet sky radiances. The measured radiances are obtained by a polarization-insensitive modified Brewer double spectrometer located at Goddard Space Flight Center, in Greenbelt, Maryland, USA. Results demonstrate that the Brewer angular (0–72° viewing zenith angle) and spectral (303–320 nm) measurements of sky radiance in the solar principal plane provide sufficient information to derive tropospheric ozone diurnal variability. In addition, the Brewer measurements provide stratospheric ozone vertical distributions at least twice per day near sunrise and sunset. Frequent measurements of total column ozone amounts from direct-sun observations are used as constraints in the retrieval. The vertical ozone profile resolution is shown in terms of averaging kernels to yield at least four points in the troposphere–low stratosphere, including good information in Umkehr layer 0 (0–5 km). The focus of this paper is on the derivation of stratospheric and tropospheric ozone profiles using both simulated and measured radiances. We briefly discuss the necessary modifications of the Brewer spectrometer that were used to eliminate instrumental polarization sensitivity so that accurate sky radiances can be obtained in the presence of strong Rayleigh scattering and aerosols. The results demonstrate that including a site-specific and time-dependent aerosol correction, based on Brewer direct-sun observations of aerosol optical thickness, is critical to minimize the sky radiance residuals as a function of observing angle in the optimal estimation inversion algorithm and improve the accuracy of the retrieved ozone profile.

Citation: Tzortziou, M., N. A. Krotkov, A. Cede, J. R. Herman, and A. Vasilkov (2008), A new technique for retrieval of tropospheric and stratospheric ozone profiles using sky radiance measurements at multiple view angles: Application to a Brewer spectrometer, *J. Geophys. Res.*, 113, D06304, doi:10.1029/2007JD009093.

1. Introduction

[2] Ozone (O₃) is a critical atmospheric constituent that is involved in the photochemistry of both the troposphere and stratosphere and in shielding the Earth's surface from Ultraviolet-B (UV-B) radiation (280–320 nm). In addition to regulating the oxidation capacity of the lower atmosphere and influencing background levels of trace chemicals, O₃ is an important greenhouse gas, affecting radiative balance and global climate. Ozone absorption in the UV-B region of

the solar spectrum affects many photochemical and biological processes. Variations in O₃ concentration affect the amount and spectral properties of surface UV radiation with far-reaching consequences for both terrestrial and aquatic ecosystems [e.g., Diffey, 1991; Tevini, 1993]. Increased ground-level O₃ concentrations are toxic upon inhalation or contact, posing serious threats to agricultural productivity and human health. The vertical distribution of O₃ in the troposphere typically shows strong seasonal and diurnal variability, especially in polluted urban areas where there is often more tropospheric O₃ in the afternoon as photochemical smog builds up [Taubman *et al.*, 2006]. Thus, frequent (e.g., hourly) measurements of tropospheric O₃ concentrations and vertical distribution are essential for determining short timescale changes in O₃ amounts close to the ground, and quantifying the role of tropospheric O₃ on local and regional environmental degradation, tropospheric chemistry, surface UV-B levels, human health and radiative forcing.

[3] Two main techniques have been available for measuring tropospheric O₃ at high vertical resolution: (1) in situ sensing from balloon sondes and aircraft [e.g., Thompson *et*

¹Earth System Science Interdisciplinary Center, University of Maryland, College Park, Maryland, USA.

²NASA Goddard Space Flight Center, Greenbelt, Maryland, USA.

³Goddard Earth Science and Technology Center, University of Maryland, Baltimore County, Baltimore, Maryland, USA.

⁴Science Systems and Applications Incorporated, Lanham, Maryland, USA.

al., 2003; Taubman et al., 2006] and (2) remote sensing using active ozone-lidar techniques [e.g., Browell et al., 1985; Uthe et al., 1992; McGee et al., 1995]. As these measurement approaches are typically associated with high maintenance and operational labor costs, they are not suited for long-term hourly measurements at multiple sites. Moreover, active ozone-lidar techniques usually do not detect changes in the lower troposphere (altitudes below 7 km), and are limited to night, early morning, and late evening observations [McDermid et al., 1995, 2002; McGee et al., 1995]. Several passive remote sensing techniques have been developed for obtaining information on O₃ vertical distribution from satellites and ground-based observations. The ground-based Umkehr technique [e.g., Mateer, 1965; Petropavlovskikh et al., 2005] provides information on stratospheric and limited information on upper tropospheric O₃ profiles using measurements of zenith-sky UV radiances at different solar elevations. Umkehr observations are restricted to measurements near sunrise and sunset (Solar Zenith Angles, SZAs, between 60° and 90°) and last approximately 2 h, during which significant changes in atmospheric conditions can occur, causing O₃ retrieval errors. Satellite nadir-viewing (e.g., Solar Backscatter Ultraviolet, SBUV, Global Ozone Monitoring Experiment, GOME, and Scanning Imaging Absorption Spectrometer for Atmospheric Cartography, SCIAMACHY) and limb-viewing (e.g., Stratospheric Aerosol and Gas Experiment, SAGE, and SCIAMACHY) observations can derive only one O₃ profile, or tropospheric column O₃ amount, per day using optimal estimation theory [e.g., Hoogen et al., 1999; Rault, 2005; Palm et al., 2005; Liu et al., 2007] or residual-based approaches [e.g., Fishman et al., 1990; Ziemke and Chandra, 1999; Schoeberl et al., 2006; Ziemke et al., 2006]. All of the above passive techniques have little sensitivity to ozone changes close to the ground (e.g., boundary layer ozone pollution) and cannot report on diurnal changes.

[4] This paper discusses and applies a new practical method for retrieving day-to-day variability in stratospheric O₃ profiles, and both seasonal and diurnal variability in tropospheric O₃ vertical distribution. Data are obtained from sky radiances measured at five Viewing Zenith Angles, VZAs, (0–72°) and six UV-B wavelengths (303–320 nm) using a modified, commercially available, Brewer double spectrometer [Kerr et al., 1985]. Brewer spectrometers are widely used all over the world for accurate measurements of solar direct and global irradiance and zenith sky radiances, as well as retrievals of total column O₃, sulfur dioxide, SO₂, and nitrogen dioxide, NO₂, amounts [e.g., Kerr et al., 1988; Cede and Herman, 2005; Cede et al., 2006a].

[5] The technique described in this paper is based on Radiative Transfer (RT) modeling results showing that the effect of an ozone change on the sky radiance measured at the ground depends on the altitude of the ozone change, the solar and viewing zenith angle of the measurement, and the wavelength. RT calculations demonstrate that there is sufficient information in the Brewer angular and spectral sky radiances measured throughout the day to determine tropospheric O₃ profile diurnal variability with frequency up to 30 min. On the basis of averaging kernel analysis, Brewer measurements at large SZAs (>75°) can provide additional information on stratospheric O₃ vertical distributions at least

twice per day, near sunrise and sunset. At large SZAs, the technique described here provides an improved alternative to the traditional Umkehr technique [Mateer, 1965; Petropavlovskikh et al., 2005]. The two improvements are (1) that the measurement only takes a few minutes (compared to approximately 2 h in the Umkehr method) and (2) that the retrieval has better vertical resolution in the lower stratosphere (i.e., Umkehr layer 3).

[6] The retrieval method uses an optimal estimation approach [Rodgers, 2000] to invert Brewer radiance measurements and retrieve O₃ profiles. Climatological a priori information, obtained by combining satellite ozone data with data from balloon ozonesondes [McPeters et al., 2007], and total column O₃ amounts, derived by nearly simultaneous direct-sun Brewer observations, were used to stabilize and constrain the retrieval. The optimal estimation O₃ profile retrieval approach has been discussed previously in theory-only studies. Liu et al. [2006] demonstrated the possibility and information content of retrieving tropospheric O₃ at a solar zenith angle of 45°, using synthetic downwelling UV spectral radiances (300–340 nm), neglecting polarization, and assuming a cloud-free and aerosol-free sky. Guo et al. [2007] recently presented a method for retrieving O₃ profiles from simulated sky polarization data (300–345 nm) obtained from a virtual ground-based spectrometer at 0.2-nm spectral resolution (226 channels used in their retrieval) and a signal-to-noise ratio better than 500 at all wavelengths. As mentioned by Guo et al. [2007], their synthetic retrieval was conducted with very specific geometry and parameterization and for perfectly known atmospheric temperature and aerosol profiles, which is unlikely to be true for real cases.

[7] The radiative transfer study and data analysis presented here is the first practical tropospheric O₃ profile retrieval that applies the optimal estimation method to a dynamic atmosphere (that includes changing O₃, aerosols and trace gas amounts) and to the data and technical characteristics of an existing class of ground-based spectrometers. Currently, there are more than 50 Brewer double spectrometers operating worldwide that could be adapted for this technique, with the majority in Canada, the US, and Europe. Modification of the Brewer instrument is necessary to eliminate instrumental polarization sensitivity so that accurate sky radiances can be obtained in the presence of aerosols.

[8] The emphasis in this paper is on the development and optimization of the tropospheric O₃ inversion algorithm, as applied to the technical characteristics of the Brewer instrument (section 2) and information content analysis of simulated Brewer sky radiance data (sections 3.1–3.2). Section 3.3 discusses the application of the retrieval to measurements obtained from the modified Mark III Brewer double spectrometer located at Goddard Space Flight Center (GSFC) in Greenbelt, Maryland, USA (38.98°N, 76.83°W). Results demonstrate that including a measured site-specific and time-dependent aerosol correction is critical to achieving an accurate fit to the sky radiance spectra and O₃ retrieval. Extending the technique to include longer wavelengths (i.e., $\lambda > 320$ nm) could provide information on both O₃ vertical distribution and aerosol properties. In this study, the aerosol optical properties (e.g., Aerosol Optical Thickness, AOT,



Figure 1. A photograph of the modified Mark III Brewer double spectrometer (#171) at NASA GSFC site in Greenbelt, Maryland, showing the modified curved radiance entrance port on the bottom right.

and Single Scattering Albedo, SSA) were not included as part of the retrieved state vector, but were considered as nonretrieved forward model parameters that were applied as a dynamic correction. A detailed sensitivity study on the effects of uncertainties in the measured aerosol properties on the O₃ retrieval is presented in section 3.4.

2. Methodology

2.1. Brewer Instrument

[9] In its various models, the Brewer spectrometer [e.g., Kerr *et al.*, 1985] has been available for almost 25 years as a means of making accurate measurements of solar irradiance and zenith sky radiances, which can then be used to derive total column O₃, SO₂, and NO₂ amounts [Kerr *et al.*, 1988; Fioletov *et al.*, 1998; Cede and Herman, 2005; Cede *et al.*, 2006a]. A newer version, the Mark-III Brewer double spectrometer, has been used to derive more accurate total column O₃ and SO₂ with the advantage of a very low internal stray light fraction ($<10^{-7}$) at the short UV-B wavelengths. The very low instrumental stray light makes the Mark III Brewer ideal for measuring sky radiances in the UV spectral region except for the problem of polarization sensitivity related to the grating and to the flat quartz entrance window (Fresnel effect) covering the entrance port [Cede *et al.*, 2006b]. To eliminate both sources of polarization sensitivity so that accurate sky radiances can be obtained in the presence of aerosols, our Mark III Brewer instrument (#171) was modified in 2004 by introducing a depolarizer in front of the grating and by installing a curved quartz window such that the measured incident radiation is always perpendicular to the window surface (Figure 1).

[10] The Brewer #171 double monochromator has a wavelength range from 282.6 to 363.6 nm and an approximately triangular slit function with full width at half maximum from 0.47 to 0.67 nm that decreases with increasing wavelength. In the initial data reduction, raw counts of the Brewer are converted to “effective count rates,” which includes the laboratory radiometric calibration, corrections for the dark count, the internal attenuation

by neutral-density filters used to adjust the intensity reaching the detector, the dead time of the photomultiplier tube, and the instrument’s temperature dependence. The narrow field-of-view port of Brewer #171 is absolutely calibrated in our laboratory using the method described by Kazadzis *et al.* [2005].

[11] The Brewer can operate either in a “scanning mode,” where the gratings are moved and any wavelength can be selected, or in a “slit mask mode,” which allows nearly simultaneous measurements at six wavelengths that are about 3 nm apart at fixed grating positions. In the slit mask mode, the measured signals are obtained from multiple runs over all six wavelengths. In the solar plane, sky radiance measurements are obtained with a total integration time of ~ 0.5 s at each wavelength and each VZA. For total column O₃ retrievals [Kerr *et al.*, 1981] and trace gases (SO₂ and NO₂) [Cede *et al.*, 2006a], the Brewer is operated in direct-sun viewing mode.

[12] The Brewer direct-sun UV irradiance measurements can also provide information on AOT at various wavelengths between 303 and 363 nm [Carvalho and Henriques, 2000; Groebner *et al.*, 2001; Cheymol and De Backer, 2003; Bais *et al.*, 2005; Kazadzis *et al.*, 2005]. The Brewer spectrometer at GSFC has always operated in conjunction with Cimel Sun photometers (reference instruments of NASA AERONET network: <http://aeronet.gsfc.nasa.gov> [Holben *et al.*, 1998]) that provide additional aerosol information (e.g., AOT, particle size distribution (PSD) and SSA at visible wavelengths $\lambda > 440$ nm) [e.g., Dubovik *et al.*, 2002]. In addition, the Brewer at GSFC operates in conjunction with a UV Multifilter Rotating Shadowband Radiometer (MFRSR) that measures total column O₃ [Slusser *et al.*, 1999; Gao *et al.*, 2001], and AOT and SSA in the UV [Krotkov *et al.*, 2005a, 2005b]. The UV-MFRSR was recently modified to add a 440 nm channel so as to overlap the Cimel almucantar inversions [Dubovik *et al.*, 2002] and provide information on the spectral dependence of SSA values eliminating a potentially incorrect extrapolation from the visible range [Krotkov *et al.*, 2007].

[13] The tropospheric O₃ retrieval described here uses spectral and angular sky radiances in the solar principal plane measured at the Brewer’s #171 six wavelengths at the standard ozone slit mask position (303.22, 306.32, 310.06, 313.50, 316.79, 319.98 nm). Because aerosol forward scattering within the solar aureole affects the accuracy of the Brewer measurements, only sky radiances measured at the anti-sun direction were used in the retrieval. Measurements in the solar plane anti-sun direction are performed at five VZAs (0, 18, 36, 54, 72°). A complete scan of the principal plane (solar and antisolar directions) is made every ~ 30 min throughout the day. The random noise standard deviations in the Brewer UV radiances ($\pm\sigma_N$, see Table 1) are typically larger for shorter wavelengths, larger VZAs, and larger SZAs. In addition to random noise, absolute sky radiances measured by the Brewer instrument are estimated to have approximately a 2% uncertainty (1 sigma). A small fraction of the uncertainty ($\sim 0.5\%$) is due to the wavelength calibration and wavelength stability of the instrument, which affects each wavelength differently. The larger fraction of the uncertainty is in the absolute radiometric laboratory calibration, affecting all wavelengths approximately in the same

Table 1. Random Noise (2-Sigma) in Brewer Radiances, Estimated as the Average of Data Obtained at the GSFC Site in 2005^a

SZA (deg)	VZA	Wavelengths (nm)					
		303	306	310	313	316	320
75	72	3.18	1.66	0.83	0.48	0.33	0.30
75	54	3.32	1.71	0.85	0.49	0.34	0.30
75	36	3.35	1.66	0.82	0.46	0.31	0.30
75	18	3.51	1.64	0.77	0.42	0.30	0.30
75	0	4.04	1.82	0.81	0.43	0.30	0.30
45	72	1.10	0.76	0.57	0.40	0.31	0.30
45	54	1.18	0.84	0.62	0.41	0.35	0.30
45	36	1.25	0.86	0.62	0.41	0.38	0.31
45	18	1.25	0.86	0.62	0.41	0.33	0.30
45	0	1.30	0.87	0.61	0.40	0.31	0.30

^aOnly SZA = 45° and SZA = 75° are shown here. The 2-sigma noise in Brewer data is in %.

way. This bias can largely be removed by normalizing the measured radiance spectra to measurements at a specific VZA or a specific wavelength. To minimize the effect of the calibration bias, the O₃ retrieval was performed after normalizing all radiances in the five shortest-wavelength slit mask positions (303.22–316.79 nm) to the radiances measured at 319.98 nm, which is the least affected by changes in O₃. Reducing the number of independent wavelengths from six to five increases the statistical noise in the retrieval, but improves the accuracy.

2.2. Tropospheric Ozone Inversion Algorithm

[14] The inversion strategy for O₃ profile retrieval uses a forward RT model to simultaneously fit Brewer angular and spectral measurements of sky radiance, $I(\text{VZA}, \lambda)$, constrained by the nearly simultaneous Brewer direct-sun total column ozone measurement, TCO. The TCO measurement is practically independent of the ozone profile shape at SZAs less than 80°. The inversion algorithm is based on the optimal estimation approach [Rodgers, 2000], and uses climatological a priori O₃ profile information [McPeters *et al.*, 2007] to stabilize the retrieval. The basic equations used are:

$$\begin{aligned} \mathbf{y} &= \mathbf{f}(\mathbf{x}) + \boldsymbol{\varepsilon}_y \\ \mathbf{x}^a &= \mathbf{x} + \boldsymbol{\varepsilon}_a \end{aligned} \quad (1)$$

Here, solar-normalized sky measurements or N values, defined as $N(\text{VZA}, \lambda) = -100 \log_{10}[I(\text{VZA}, \lambda)/F]$, where F is the solar irradiance (ATLAS-3 SUSIM solar spectrum convolved with the measured wavelength-dependent Brewer slit functions and corrected to the actual Sun–Earth distance), are combined with the Brewer measurement of TCO into a single measurement vector, \mathbf{y} . As mentioned in section 2.1, Brewer measurements in the five shortest-wavelength slit mask positions (303.22–316.79 nm) were normalized to those at 319.98 nm to minimize systematic errors in sky radiances (both from the model and measurements). The retrieval assumes that residual random errors have a Gaussian distribution about the mean with known covariance matrix \mathbf{S}_y (covariance matrix has only diagonal elements, Table 1). To constrain the retrieval to

only positive ozone values, the state vector \mathbf{x} is defined as the natural logarithm of the ozone amount, ω_j , in the standard Umkehr layer j : $\mathbf{x} = [\mathbf{x}_j] = [\ln(\omega_j)]$, for $j = 0:10$ [0–5, 5–10, 10–15, 15–20, ..., 45–50 km]. The measurements are constrained with the a priori ozone profile; $\boldsymbol{\varepsilon}_a$ is the error in the a priori ozone profile \mathbf{x}^a with covariance matrix \mathbf{S}_a [McPeters *et al.*, 2007] (see also discussion below).

[15] According to the optimal estimation approach, the statistically best solution that can be derived from all given data is a vector \mathbf{x}_o corresponding to the minimum of the following quadratic form (cost function with regularization term):

$$\Psi(\mathbf{x}) = (\mathbf{y} - \mathbf{f}(\mathbf{x}))^T \mathbf{S}_y^{-1} (\mathbf{y} - \mathbf{f}(\mathbf{x})) + (\mathbf{x}_a - \mathbf{x})^T \mathbf{S}_a^{-1} (\mathbf{x}_a - \mathbf{x}) \quad (2)$$

Minimization of the cost function $\Psi(\mathbf{x})$ is implemented using Gauss-Newton iterations of a linearized approximation \mathbf{K} of the forward model $\mathbf{f}(\mathbf{x})$ at each iteration step:

$$\mathbf{x}_{p+1} = \mathbf{x}_p + \mathbf{S}_{p+1} [\mathbf{K}_p^T \mathbf{S}_y^{-1} (\mathbf{y} - \mathbf{f}(\mathbf{x}_p)) + \mathbf{S}_a^{-1} (\mathbf{x}_a - \mathbf{x}_p)] \quad (3)$$

where, $\{\mathbf{K}_p\}_{i,j} = \{\partial \mathbf{f}(\mathbf{x})\}_i / \partial \mathbf{x}_j|_{\mathbf{x}_p}$ is the Jacobian weighting function matrix of the partial derivatives (sensitivity of the forward model F to the state \mathbf{x}) in the near vicinity of the vector \mathbf{x}_p and $\mathbf{S}_{p+1} = (\mathbf{K}_p^T \mathbf{S}_y^{-1} \mathbf{K}_p + \mathbf{S}_a^{-1})^{-1}$ is the solution error covariance matrix. The partial derivative elements for sky radiances \mathbf{K}_p are recalculated numerically at each iteration step by finite differencing forward model calculated N_i values (TOMRAD code, see section 2.3) with respect to logarithms of the layer ozone amounts. The iteration starts with some initial estimate of the state \mathbf{x}_{in} and continues until the convergence is satisfied when both the norm of the vector $\Delta \mathbf{x}^p$ (difference between iterations) and the cost function increment become less than specified threshold values (i.e., 0.3% change in the cost function). It should be noted here that forward calculations are done for all orders of scattering, as compared with traditional Umkehr retrieval forward model, where only single scattering is recalculated at each step and multiple scattering is taken from the look-up tables while it is still adjusted for ozone profile change.

2.2.1. A Priori Ozone Information

[16] The optimal estimation approach [Rodgers, 2000] uses climatological a priori information to stabilize the retrievals. The O₃ climatology used in this paper, was derived by combining data from the SAGE II instrument on the ERBS satellite and the Microwave Limb Sounder (MLS) instrument on UARS satellite with data from balloon ozonesondes [McPeters *et al.*, 2007]. This climatology was produced for use with the Version 8 Total Ozone Mapping Spectrometer (TOMS) and SBUV ozone profile retrieval algorithms. For the inversion of simulated Brewer data (section 3.1), the a priori O₃ profile and covariance matrix, \mathbf{S}_a , were derived from the climatology for latitude zone 30–40°N and the month of January. For the inversion of Brewer measurements obtained on 23 July 2005 (section 3.3), an ozone climatology for the latitude zone 30–40°N and the month of July was used. Because the ozone retrieval method described here is particularly sensitive to changes in tropo-

spheric O₃, especially at small SZAs, the a priori constraint is relaxed in the first three Umkehr layers by increasing the a priori standard deviation (similarly as described by *Liu et al.* [2006]). However, for retrievals at small SZAs, a strong a priori constraint is forced for stratospheric layers, because the small-SZA observations are not very sensitive to changes in stratospheric ozone. The retrieval assumes no a priori correlations between O₃ layers (zero off-diagonal elements of \mathbf{S}_a).

2.2.2. Error Estimate

[17] The solution error covariance could be split between smoothing and retrieval errors [Rodgers, 2000]:

$$\hat{\mathbf{x}} \approx \mathbf{x}_0 + (\mathbf{A} - \mathbf{I})(\mathbf{x}_0 - \mathbf{x}_a) + \mathbf{G}_y \varepsilon_y \quad (4)$$

The smoothing error is defined by the averaging Kernel matrix $\mathbf{A} = \mathbf{G}_y \mathbf{K}_x$, which represents the sensitivity of the retrieved state $\hat{\mathbf{x}}$ to the perturbations in the true state \mathbf{x}_0 (\mathbf{I} is identity matrix in state space) and the a priori ozone statistics (covariance matrix). Since ozone profile statistics are not known at the GSFC site, no attempt was made to characterize the smoothing error here, considering the retrieval as an estimate of the smoothed true ozone profile [Rodgers, 2000]. The retrieval error is given by the $\mathbf{G}_y \varepsilon_y$ term, where $\mathbf{G}_y = \mathbf{S}_{p+1} \mathbf{K}_p^T \mathbf{S}_y^{-1}$ is the gain matrix and ε_y is calculated from estimates of the Brewer measurement noise (see Table 1), neglecting forward RT model errors (TOMRAD RT code [Dave, 1964]). The forward RT model errors are not expected to be significant, since the algorithm uses an accurate vector treatment of sky radiance multiple scattering for exact observational geometry and realistic aerosol corrections based on colocated and nearly simultaneous ancillary measurements of aerosol optical properties (see section 2.3). Thus, the covariance of the retrieval noise is determined by Brewer measurement noise, $\mathbf{S}_m = \mathbf{G}_y \mathbf{S}_e \mathbf{G}_y^T$, where the Brewer measurement noise covariance matrix \mathbf{S}_e is assumed diagonal with variances shown in Table 1.

2.3. Forward Radiative Transfer Models and Data Simulation

[18] The auxiliary equations method, which accounts for all orders of scattering and polarization effects (TOMRAD RT code [Dave, 1964]), was used as a forward model to calculate radiances and weighting functions during the retrieval process. The TOMRAD RT code assumes a horizontally homogeneous Rayleigh atmosphere with a specified O₃ profile, neglecting the effects of aerosols. The pseudo-spherical geometry correction (no refraction) was applied to the direct solar irradiance. Forward model calculations were performed using O₃ and temperature profiles, spline interpolated to 101 pressure layers (20 equal logP layers per decade of pressure). The O₃ absorption coefficients estimated for the GOME satellite instrument [Burrows et al., 1999] were used, along with the Rayleigh scattering coefficients and depolarization factors [Bates, 1984], slit-averaged using measured Brewer slit functions and weighted using ATLAS-3/SUSIM solar flux.

[19] The TOMRAD RT code was also used to simulate Brewer measurements for a pure Rayleigh scattering atmosphere. Surface albedo was fixed equal to 0.02 at all wavelengths. Simulations were performed for the Brewer's six

wavelengths (303.22–319.98 nm), for five Brewer VZAs (0–72°) in the solar plane, and various SZAs (<75°). Estimated random noise, based on the 1-sigma error observed in the Brewer total column O₃ amount (~0.5%) and the Brewer UV radiances ($\pm\sigma_N$, see Table 1), was applied to the synthetic measurement vector. The random noise applied to the simulated radiances was estimated for each wavelength, VZA and SZA, as the average noise of all measured data obtained in 2005. Ozone retrievals were repeated for 10 independent realizations to estimate error propagation from random noise to the retrieval (see section 3.1).

[20] Since the TOMRAD RT model does not allow for aerosol scattering, the University of Arizona Gauss-Seidel, pseudo-spherical polarized RT code [Herman et al., 1995] was used to simulate Brewer measurements for a real atmosphere that includes both O₃ and aerosols, and to calculate aerosol corrections during the retrieval process. The interface to the Arizona code and specification of the background atmosphere were modified to match that of the TOMRAD code and ensure that the two codes were in agreement (<0.1%) for a pure Rayleigh scattering atmosphere. Time-dependent and site-specific aerosol optical models were constructed using Brewer direct-sun measurements of AOT in the spectral range 303 to 320 nm. Brewer AOT were corrected for gaseous absorption from O₃ and NO₂ and agreed, within specified uncertainty (i.e., better than ~0.02), with spectrally extrapolated AOT from AERONET network-reference Sun photometers. The aerosol size distribution was derived from AERONET almucantar inversions [Dubovik et al., 2002]. The aerosol SSA in the UV-B wavelength region, which cannot be obtained from AERONET, was estimated from the measurements of global and diffuse atmospheric transmittances measured by a UV-MFRSR instrument [Krotkov et al., 2005b, 2007]. Aerosol vertical distributions in the boundary layer were chosen in agreement with micropulse lidar measurements at Goddard (MPL net, <http://mplnet.gsfc.nasa.gov/>).

[21] The aerosol correction was calculated by running the Arizona RT code for two cases, one for a pure Rayleigh atmosphere and the second with aerosols added to the model. The runs were made with the exact measurement geometry (SZAs and VZAs) and an a priori O₃ profile scaled to the total column ozone amount measured by the Brewer. The correction was applied to the TOMRAD calculated radiances at each iteration step. For small amounts of aerosols (e.g., AOT₅₀₀ = 0.23, typical clear day at the GSFC site [Dubovik et al., 2002]), there is little effect on the weighting functions, but significant effect on the sky radiances and O₃ retrieval. This procedure allows the much faster TOMRAD RT model to be used directly in the retrieval algorithm.

[22] Corrections for the Ring effect were not included in the retrievals shown below. Preliminary calculations demonstrated that this effect has little impact on the O₃ retrieval at all Brewer wavelengths except 310 nm (data not shown here). Results showed that the retrieval method works well even when information at 310 nm is not included (see section 3.1). If necessary, normalization of sky radiances to zenith direction [Liu et al., 2006] practically eliminates the Ring effect, at the cost of reducing stratospheric information content of the measurements. Zenith normalization did not

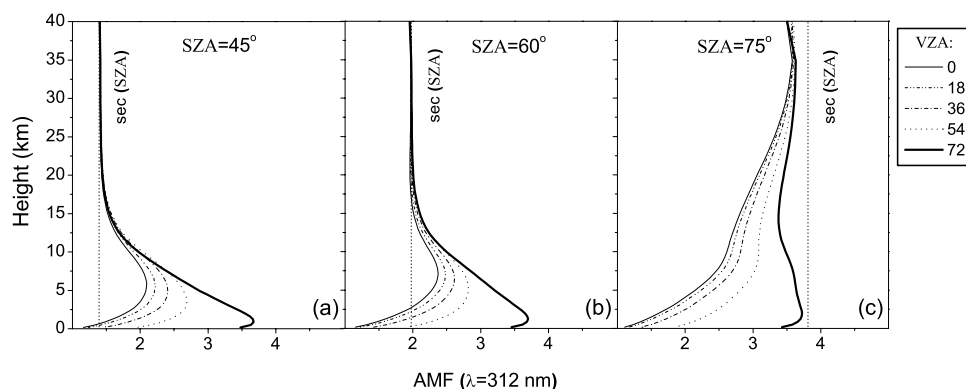


Figure 2. The Air Mass Factor for (a) SZA = 45°, (b) SZA = 60°, and SZA = 75°. Results are shown at 312 nm and five VZAs (0, 18, 36, 54, and 72). The dotted line is the value of the geometrical path ($\sim \sec(\text{SZA})$).

significantly change the retrieved tropospheric ozone values, but increased the random noise in the retrieval. The algorithm presented here does not use zenith sky normalization.

3. Results and Discussion

3.1. Inversion Characterization

3.1.1. Air Mass Factor

[23] The air mass factor, AMF, concept was used to examine the sensitivity of the sky radiance measurements to relative changes in O₃ amount in a given vertical layer. The AMF can be expressed as the ratio of the fractional change in logarithm of sky radiance at a specific wavelength and VZA, $\Delta \ln(I_i(x))$, when the O₃ absorption optical thickness in a certain layer j is perturbed by a small amount $\Delta \tau_j$, to $\Delta \tau_j$: $\text{AMF}_{ij} = \Delta \ln(I_i(x)) / \Delta \tau_j$ [Liu *et al.*, 2005]. In general, a larger AMF in a layer means increased sensitivity to ozone change. The calculated AMFs are shown in Figure 2 for Brewer measurements at 312 nm, five VZAs in the solar plane (0, 18, 36, 54, 72°) and three SZAs (45, 60 and 75°).

[24] At 45° SZA and VZA = 0° (Figure 2a), the AMF increases with decreasing altitude reaching a maximum value at about 6 km (or, within Umkehr layer 1). This suggests that zenith sky measurements at SZA = 45° are most sensitive to O₃ changes at this altitude. As SZA increases, zenith sky measurements become more sensitive

to higher altitudes (i.e., maximum value at 7 km for SZA = 60°, Figure 2b). As the VZA increases, the altitude of maximum AMF decreases and the absolute value of AMF increases, suggesting that measurements at large VZAs (i.e., 72°) become increasingly sensitive to O₃ changes closer to the surface (Figures 2a and 2b). At altitudes higher than Umkehr layer 4 (20 to 25 km), the AMFs are the same for all VZAs and equal to the estimated geometrical path (indicated in Figure 2 as the vertical dashed line). This means that there is no additional information about stratospheric O₃ in multiple angle sky measurements at small to moderate SZAs less than approximately 60°. The results presented here for SZA = 45° are consistent with Liu *et al.* [2006, Figure 2a].

[25] At SZA = 75° (Figure 2c) and VZAs smaller than ~54°, the AMF increases with increasing altitude suggesting that Brewer sky measurements at large solar zenith angles are sensitive to stratospheric O₃ changes. Moreover, Brewer measurements at large VZAs (e.g., 72°) are equally sensitive to O₃ changes in the lower troposphere regardless of SZA (Figures 2a and 2b), suggesting that Brewer sky measurements at different SZAs can provide information on diurnal changes in surface O₃ amounts.

3.1.2. Averaging Kernels

[26] The averaging Kernel matrix $\mathbf{A} = \mathbf{G}_y \mathbf{K}_x$, represents the sensitivity of the retrieved state $\hat{\mathbf{x}}$ to the perturbations in

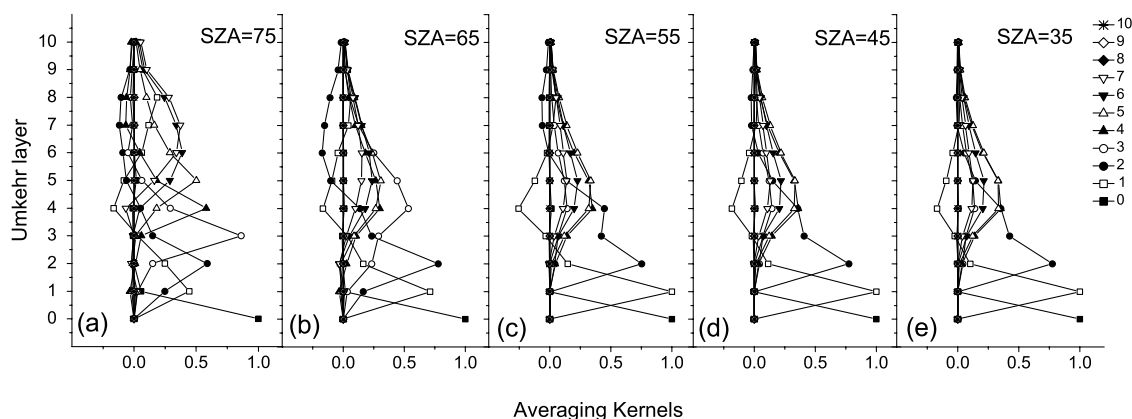


Figure 3. Averaging Kernels at SZAs (a) 75°, (b) 65°, (c) 55°, (d) 45°, and (e) 35°.

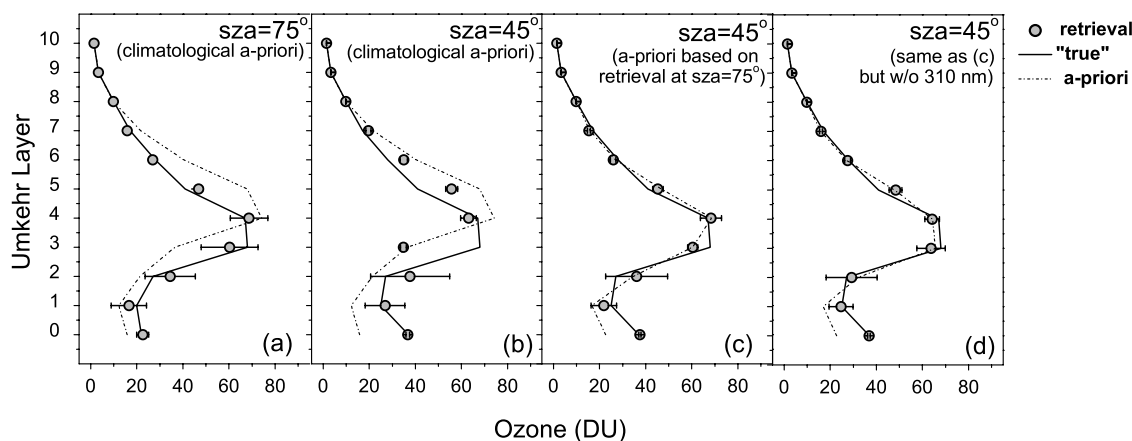


Figure 4. Climatological a priori (dashed line), “true” (solid line), and retrieved (circles) O₃ profiles for retrievals at (a) SZA = 75° and (b) SZA = 45°. (c) Retrieval at SZA = 45° using the Brewer measurements at the beginning of the day (i.e., SZA = 75°) as a priori O₃ information to constrain O₃ in the stratosphere. (d) Same as Figure 4c but retrievals at SZA = 75° and SZA = 45° were performed without including the 310 nm wave band. The horizontal bars represent one standard deviation in the retrieval resulting from the measured noise in simulated radiances (Table 1).

the true state \mathbf{x}_0 . The Averaging Kernels were estimated for five different SZAs in the range 35–75° (Figure 3). On the basis of these results, at relatively large SZAs (close to sunrise and sunset) the retrieval is more sensitive in the upper troposphere and lower stratosphere (Umkehr layers 2, 3) than in the middle troposphere (e.g., Umkehr layer 1) (Figure 3a). The estimated averaging kernel for Umkehr layer 3, peaks at the right altitude and is well resolved, which is an improvement over the traditional Umkehr technique where the kernel for layer 3 has significant negative excursions [e.g., Rodgers *et al.*, 1998]. Moreover, at SZA = 75°, the lower troposphere (Umkehr layer 0) is also very well resolved (retrieval sensitivity close to 1, Figure 3a). This is in agreement with our AMF calculations.

[27] As the SZA decreases (e.g., morning to noon), the sensitivity to profile shape moves downward in the atmosphere providing increasingly accurate retrievals in the lower and upper troposphere (e.g., Figures 3c–3e). At SZAs = 35–55°, Umkehr layers 0, 1, 2 are well resolved, with retrieval sensitivity close to 1 in layers 0 and 1. This means that we can expect resolved ozone points near the surface, at about 2, 7 and 12 km. These results are in agreement with the calculations of AMF shown in Figures 2a and 2b for SZAs 45° and 60°.

[28] The midlatitude stratospheric O₃ profile shape is assumed approximately constant from sunrise to sunset. Thus, information on stratospheric O₃ obtained at the beginning or end of the day (e.g., SZA = 75–85°) can be used as a priori knowledge to constrain stratospheric O₃ for the retrievals at smaller SZAs when the sky measurements are not as sensitive to O₃ changes at high altitudes (Figure 2). Hourly retrievals at SZAs smaller than ~75° can then be used to track diurnal tropospheric variability in O₃. On days when this assumption fails, as whenever a stratospheric plume of equatorial air moves toward higher latitudes, the lower tropospheric retrieval will still be accurate, but the middle troposphere and lower stratosphere will not. The overall error will be constrained by the hourly, accurate measurement of total column ozone amount.

3.1.3. Ozone Retrieval Tests

[29] To test the retrieval method performance and subsequently optimize the inversion algorithm, retrievals were initially performed using simulations of Brewer measurements derived as described in section 2.3. Ozone retrievals were performed at large (75°) and relatively small (45°) SZAs. To demonstrate the sensitivity of the retrieval at different altitudes, simulations were performed for an atmosphere with an assumed “true” O₃ vertical distribution that was different (see Figure 4) from the climatological O₃ profile in all Umkehr layers. In addition, the simulations included some diurnal variation in the “true” total column ozone and tropospheric O₃ amounts. At SZA = 75° “true” O₃ values were 22 and 20 DU in Umkehr layers 0 and 1, respectively, and TCO was 305 DU. At SZA = 45° “true” O₃ was 37 and 25 DU in Umkehr layers 0 and 1, respectively, and TCO was 325 DU. Stratospheric O₃ in the “true” profiles was kept constant throughout the day. As shown in Figure 4, retrieval results were consistent with expectations based on the results of air mass factor and averaging kernel calculations.

[30] For the retrieval at SZA = 75° (Figure 4a), the climatological O₃ profile was used as a priori information (dashed line in Figure 4a). The retrieved O₃ values in Umkehr layers 3 through 9 were in good agreement with the “true” O₃ as expected on the basis of the AMF and Averaging Kernel analyses (estimated standard deviation in the retrieval is shown as x axis error bars). These results show that at large SZAs, the retrieval method provides an improved alternative to the traditional Umkehr technique [Mateer, 1965; Petropavlovskikh *et al.*, 2005]. The two improvements are (1) that the measurement only takes a few minutes and (2) that the retrieval has better vertical resolution in the lower stratosphere (i.e., Umkehr layer 3). In addition, the SZA = 75° retrieval at Umkehr layer 0 was in good agreement with the “true” O₃ values at SZA = 75° suggesting that Brewer measurements at large SZAs can also provide accurate tropospheric O₃ information close to the Earth’s surface.

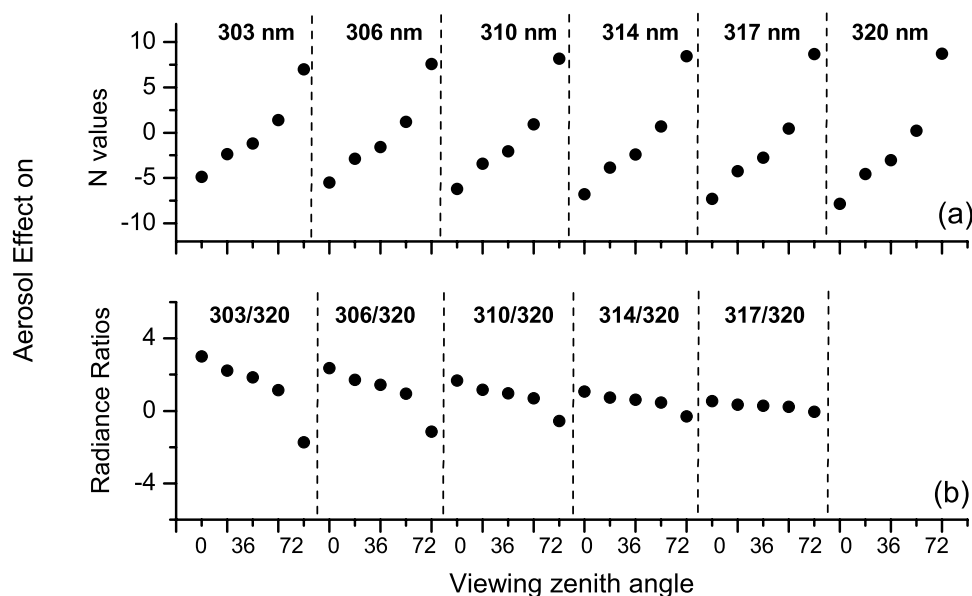


Figure 5. Effect of aerosols on (a) N values (estimated as $N_{(w-AC)} - N_{(w/o-AC)}$) and (b) radiance ratios (estimated as $\text{Rad.Ratio}_{(w-AC)} - \text{Rad.Ratio}_{(w/o-AC)}$). w-AC denotes Arizona runs for an atmosphere that includes aerosols, and w/o-AC denotes Arizona runs for same atmosphere but no aerosols. Each point corresponds to a specific VZA (0–72°) and wave band (Figure 5a), or wave band ratio (Figure 5b). Here, Brewer wavelength labels are rounded to three significant digits.

[31] An O₃ retrieval was performed for measurements at $\text{SZA} = 45^\circ$ (Figure 4b), using the climatological O₃ profile as a priori information (dashed line in Figure 4b). In this case, retrieved O₃ values, agreed well with the “true” O₃ in the first three Umkehr layers. As expected from the averaging kernels, the small SZA retrieval did not perform well in the stratosphere because most of the information at high altitudes is provided by the a priori O₃ profile. To correct this problem, the retrieval at $\text{SZA} = 45^\circ$ was performed again using the retrieval at $\text{SZA} = 75^\circ$ as a priori information to constrain O₃ at high altitudes (Figure 4c). This removes most of the effect of errors in the upper stratosphere on the retrievals at lower altitudes. Retrieved O₃ values were in good agreement with the “true” O₃ close to the ground, despite the fact that the “true” tropospheric O₃ at $\text{SZA} = 45^\circ$ was considerably different than that at $\text{SZA} = 75^\circ$ because of assumed diurnal variation. Standard deviations in the retrieval and estimated differences between retrieved and true O₃ profiles were relatively small. Similar results were obtained when the retrieval performance was examined after excluding the 310 nm wavelength to avoid possible errors due to Ring effects (Figure 4d).

3.2. Aerosol Effect

[32] One of the main objectives of this study is application of the inversion technique to a real atmosphere where both O₃ and aerosols change throughout the day and affect UV sky radiances measured from the ground. Although normalization of Brewer measurements in the five shortest-wavelength slit mask positions to 319.98 nm minimizes systematic errors in sky radiances, this normalization does not sufficiently remove the effect of aerosols. As an example, Figure 5 shows the effect of aerosols on Brewer-measured radiance ratios for a relatively clear summer atmosphere at the GSFC site. For this specific case, mea-

sured aerosol parameters were $\text{AOT}_{(500)} = 0.18$, $\text{AOT}_{(320)} = 0.41$, and $\text{SSA} = 0.94$. A typical clear day at the GSFC site has an $\text{AOT}_{(500)}$ of about 0.23 [Dubovik et al., 2002]. Calculations were performed using the Arizona RT code for $\text{SZA} = 45^\circ$, $\text{TCO} = 323$ DU, and an O₃ profile shape from the TOMS climatology for the month of July (latitude zone 30–40°N).

[33] Even for this relatively clear day, the effect of aerosols on the N values ($\Delta N = N_{(\text{aerosol})} - N_{(\text{no aerosol})}$) was of the order of $\pm 25\%$ (± 10 N values) and strongly dependent on the VZA for all wavelengths in the range 303–320 nm (Figure 5a). Normalizing N values spectrally to 319.98 nm reduced the aerosol effect to $\pm 8\%$ (± 3 N values) (Figure 5b). Further normalizing sky radiances to a specific direction (e.g., zenith sky), did not reduce the aerosol effect because of the strong VZA dependence of the sky radiances and spectral ratios. These results show that, even on apparently clear summer days, the spectral and angular dependence of aerosol scattering significantly affects the spectral and angular dependence of radiance ratios in the 303–320 nm spectral region with subsequent effects on the O₃ retrieval. Therefore, aerosol effects were explicitly included in the retrieval using the Arizona RT code and site-specific and time-dependent aerosol optical models constructed as described in section 2.3.

3.3. Ozone Retrievals Using Measured Sky Radiances

[34] The O₃ profile retrieval method was applied to measured radiances obtained by the modified double Brewer spectrometer operating at GSFC. The retrievals are shown below for data collected under cloud-free conditions on 23 July 2005. Brewer TCO during that day varied between 312 and 323 DU. The SBUV/2 TCO, measured over GSFC on 23 July 2005 ($\text{SZA} = 34^\circ$), was 312 DU. The climatological O₃ profile for the latitude zone 30–40°N and

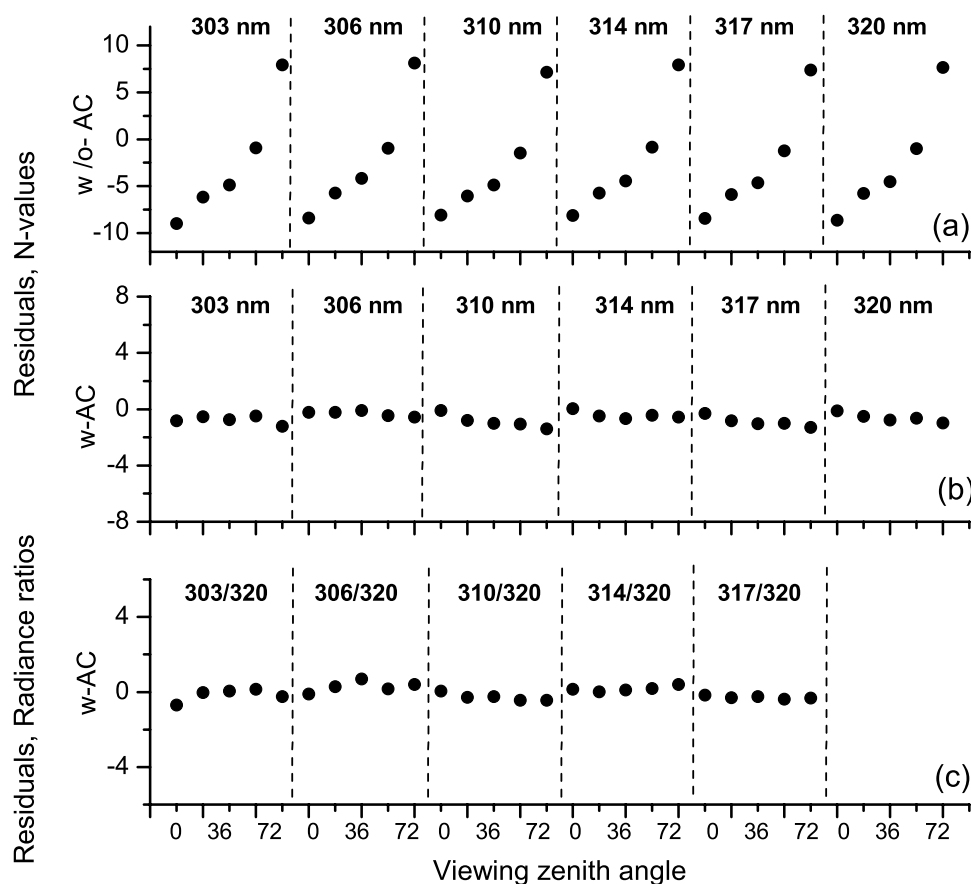


Figure 6. Residuals in N values between Brewer data (23 July 2005, SZA = 45°) and retrieval (a) without aerosol correction (w/o-AC) and (b) after correcting for the aerosol effect (w-AC). (c) Residuals in radiance ratios between Brewer data and retrieval after correcting for the aerosol effect. Each point corresponds to a specific VZA (0–72°) and wave band (Figures 6a and 6b), or wave band ratio (Figure 6c). Similar results were obtained for SZA = 75°. Here, Brewer wavelength labels are rounded to three significant digits.

the month of July [McPeters *et al.*, 2007] was used as a priori information for the retrieval at SZA = 75°. The O₃ profile retrieved from measurements at SZA = 75° was then used as an a priori for the retrievals at smaller SZAs. RT model calculations were performed for the exact values of measured Brewer wavelengths, SZAs, and VZAs to avoid look-up table interpolation errors. Information on surface pressure was derived from measurements from the nearby (5 km) USDA location in Beltsville, MD, reduced by ~2 mbar to account for the change in altitude between the Beltsville location and the GSFC Brewer location.

[35] Retrievals were initially performed for a pure Rayleigh atmosphere (Figure 6a), and then corrected for aerosols (Figures 6b and 6c). Inversion of the Brewer data without a correction for aerosols resulted in large systematic N value residuals that were (1) significantly larger than expected on the basis of the measurement errors, (2) large at all wavelengths, and (3) strongly dependent on VZA (Figure 6a; only results for SZA = 45° are shown here, qualitatively similar results were obtained for retrievals at other SZAs). The magnitude and shape of the residuals were similar to the magnitude and shape of the residuals shown in Figure 5a, indicating the presence of aerosols and the need to correct for the aerosol effect. Neglecting the effect of

aerosols in the retrieval, results in an incorrect O₃ profile that has the same effect on the calculated radiance ratios as the combined effect of ozone and aerosols present in the atmosphere. The O₃ profiles retrieved in this case are shown in Figure 7a for SZA = 45° and 75°. The retrieved O₃ profiles were considerably different than the SBUV/2 measured O₃ profile both in the troposphere (e.g., Umkehr layer 0) and in the stratosphere.

[36] Including a correction for the effect of aerosols in the inversion of the Brewer data significantly reduced the residuals in the N values (Figure 6b). The aerosol correction was estimated using the methodology described in section 2.3. Measured AOT₍₃₂₀₎, based on the Brewer direct-sun measurements, was 0.315 at SZA = 75° and 0.41 at SZA = 45°. Single scattering albedo, derived using the direct/diffuse irradiance ratio measured with the colocated UV-MFRSR, was 0.94 without large diurnal variation. The aerosol vertical distribution in the boundary layer was chosen in agreement with Micropulse lidar measurements performed during the same day at the GSFC site (lidar measurements performed during 1200–2400 UTC). Including this first-order aerosol correction in the retrieval reduced the residuals in the N values from ±10 N values (without aerosol correction) to less than ±1 N values (~2%) (results for

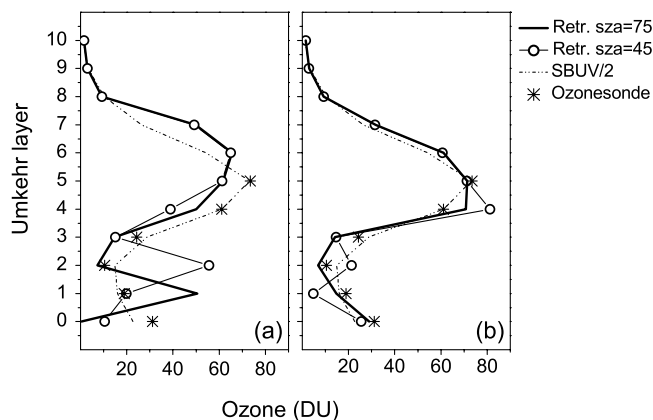


Figure 7. Ozone retrieval based on Brewer measurements from 23 July 2005 (a) for a pure Rayleigh atmosphere and (b) for the real atmosphere with aerosols. Retrievals are shown at $\text{SZA} = 75^\circ$ (using climatology as a priori information) and $\text{SZA} = 45^\circ$ (using retrieval at $\text{SZA} = 75^\circ$ as a priori information). The SBUV/2 O₃ profile and the ozonesonde measurement (average of ozonesonde measurements performed on 21 and 26 July 2005) are also shown.

$\text{SZA} = 45^\circ$ are shown in Figure 6b; similar results were obtained for retrievals at $\text{SZA} = 75^\circ$. Estimated residuals in radiance ratios, after correcting for aerosols, were less than ± 0.7 N values (Figure 6c), and in almost all cases less than the estimated Brewer measurement noise.

[37] The O₃ profiles retrieved after accounting for the effects of aerosols on the solar principle plane radiance distributions are shown in Figure 7b for SZAs 45° and 75° . Estimated O₃ amounts in the upper troposphere and in the stratosphere were in good agreement with the SBUV/2 measurements over GSFC for the same day. For $\text{SZA} = 45^\circ$, the retrieved O₃ value at Umkehr layer 2 is likely overestimated, and at layer 1, subsequently, underestimated (Figure 7b). These results are probably due to noise in Brewer measurements (see error bars in Figures 4c and 4d). The retrieved O₃ amount in Umkehr layer 0 was 26 DU at $\text{SZA} = 45^\circ$. This is consistent with ozonesonde measurements performed at nearby Beltsville, MD, which showed that O₃ amount in Umkehr layer 0 was 29 DU and 30 DU on 21 and 26 July 2005, respectively (there were no ozonesonde measurements made on 23 July 2005). However, the SBUV/2 O₃ value in Umkehr layer 0 was 22 DU, considerably lower than the ozonesonde measurements, showing that the new Brewer analysis method presented here provides an improved estimate of the ozone in the boundary layer.

[38] These results suggest that incorporation of an aerosol correction based on colocated aerosol measurements is necessary for removing the large effect of even small aerosol amounts when retrieving O₃ profiles from Brewer measurements of sky radiances.

3.4. Sensitivity of the O₃ Retrieval to Aerosol Model

[39] The sensitivity of the ozone retrieval to (1) AOT, (2) aerosol SSA, (3) aerosol PSD, and (4) aerosol plume height was examined, in order to estimate the errors in the

O₃ retrieval associated with the uncertainties in the aerosol optical model.

3.4.1. AOT

[40] The aerosol optical thickness at 320 nm, $\text{AOT}_{(320)}$, was varied between 0.4 and 0.54 (Figures 8a–8d). This change in AOT affected the viewing angle dependence of both N values (Figure 8a) and radiance ratios (Figure 8b), which then affected the absolute values of O₃ retrieved in different Umkehr layers (± 6 DU in the first 5 layers and -11 DU at layer 5; see Figures 8c and 8d). On the basis of comparisons with AERONET data, the uncertainty in the AOT values derived from the Brewer direct-sun measurements is ~ 0.02 (1-sigma). Variability in $\text{AOT}_{(320)}$ by 0.02 (i.e., from 0.40 to 0.42), affected the retrieved O₃ values by less than ± 1.5 DU in different Umkehr layers and had a negligible effect on the shape of the retrieved O₃ profile.

3.4.2. Aerosol SSA

[41] Typical variability in aerosol SSA at 325 nm during summer at the GSFC site is between 0.86 and 0.95 [Krotkov *et al.*, 2005b, their Table 1]. A change in SSA by ~ 0.04 had a noticeable effect on the absolute N values, but only a small effect on their angular dependence (Figure 8e) and on the radiance spectral ratios (Figure 8f). As a result, it had a negligible effect on the O₃ retrieval, as shown by the small differences (± 1.4 DU) in the retrieved O₃ values in each Umkehr layer and the almost identical shape of the two O₃ profiles (Figures 8g and 8h).

3.4.3. Aerosol PSD

[42] To examine the sensitivity of the retrieval to the aerosol PSD, the number fraction of coarse particles was increased by a factor of 10, keeping AOT constant. This large change in the PSD affected the viewing angle dependence of the N values (Figure 8i) and radiance ratios (Figure 8j). As a result, it also affected the retrieved O₃ (± 7 DU O₃ change in different Umkehr layers). However, O₃ in the first Umkehr layer changed by less than 3 DU (Figures 8k and 8l), while the overall shape of the retrieved O₃ profile was not affected significantly. Such a large increase in the number fraction of coarse particles would require predominantly dust aerosol, which is highly unlikely at the GSFC site. Using PSD climatology for this site [Dubovik *et al.*, 2002], the expected variability in PSD is considerably smaller, resulting in a change in O₃ by less than 1 DU in different Umkehr layers.

3.4.4. Aerosol Plume Height

[43] An assumption made in the Arizona code for the calculation of the aerosol correction concerns the vertical distribution of aerosols. To examine the sensitivity of the O₃ retrieval to the aerosol vertical profile, the retrieval was performed for two cases with significantly different aerosol distributions in the troposphere (Figures 8m–8p). In one case, the maximum aerosol amount was in the boundary layer followed by an exponential decrease with increasing altitude. In the second case, the aerosol vertical distribution was a Gaussian with a maximum at 2 km and standard deviation 1.5 km. The effect on the retrieved radiance ratios (Figure 8n) and O₃ profile (Figures 8o and 8p) was small, with differences in O₃ less than ± 2.3 DU in different Umkehr layers.

[44] These results suggest that while it is critical to include the effects of aerosols in the forward model, the O₃ retrieval is mostly sensitive to AOT. AOT can be

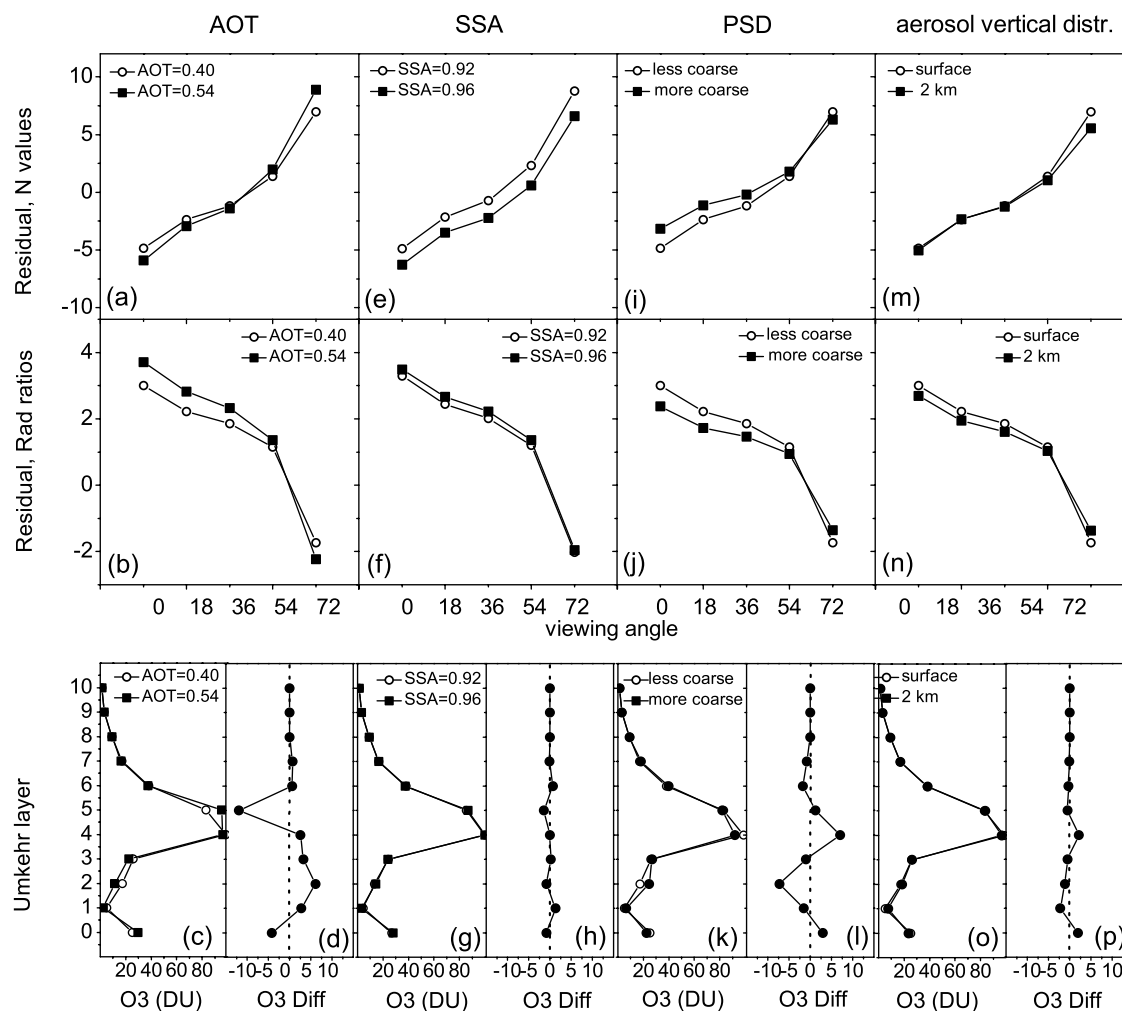


Figure 8. Effect of uncertainty in AOT, SSA, PSD, and aerosol plume height on estimated aerosol correction and O₃ retrieval. Residuals in N values are shown only at 303 nm, and residuals in radiance ratios are shown only at 303/320. Qualitatively similar results were obtained at the other wavelengths. (a) Residuals in N values (estimated as $N_{(w-AC)} - N_{(w/o-AC)}$), and (b) residuals in radiance ratios (estimated as $Ratio_{(w-AC)} - Ratio_{(w/o-AC)}$) correspond to two aerosol models with different AOT ($AOT_{(320)} = 0.4$, solid squares, and $AOT_{(320)} = 0.54$, open circles). (c) The O₃ profiles retrieved for the two different aerosol corrections. (d) Difference in retrieved O₃ values. (e–h) Similar to Figures 8a–8d but here the two aerosol models had different SSA ($SSA = 0.96$, solid squares, and $SSA = 0.92$, open circles). (i–l) Similar to Figures 8a–8d but here the two aerosol models had different aerosol particle size distribution (coarser particles, solid squares, and finer particles, open circles). (m–p) Similar to Figures 8a–8d but here the two aerosol models had different aerosol plume heights. One aerosol correction was estimated for maximum aerosol amount at the surface (open circles) and the other for maximum aerosol amount at 2 km (solid squares).

estimated with an accuracy of 0.02 (1-sigma error) from the Brewer direct-sun measurements that are performed nearly simultaneously with the sky measurements and at the same wavelengths as those used in the retrieval. Climatological values for SSA and PSD can be used to estimate a first-order aerosol correction [Arola *et al.*, 2005; Bais *et al.*, 2005; Krotkov *et al.*, 2005b, 2007]. This constrains the aerosol parameters in the forward model to sufficient accuracy for reliable tropospheric O₃ retrievals.

[45] Calculation of a specific aerosol correction using the Arizona code requires an assumption about the vertical distribution of O₃. The sensitivity of the O₃ retrieval to this

assumption was examined by running the retrieval for two different aerosol corrections that were calculated for the same aerosol model, but significantly different O₃ distributions (Figure 9e). The effect on the retrieved O₃ vertical distribution and absolute O₃ values was less than ± 3 DU at Umkehr layer 0 (Figures 9c and 9d).

[46] For the purpose of developing the algorithm, the current method of estimating the effect of aerosols on the retrievals is based on colocated aerosol measurements (e.g., using the Brewer direct-sun AOT, AERONET (PSD), MPL (vertical distribution) and UV-MFRSR (SSA)). It may be possible to obtain aerosol information directly from the

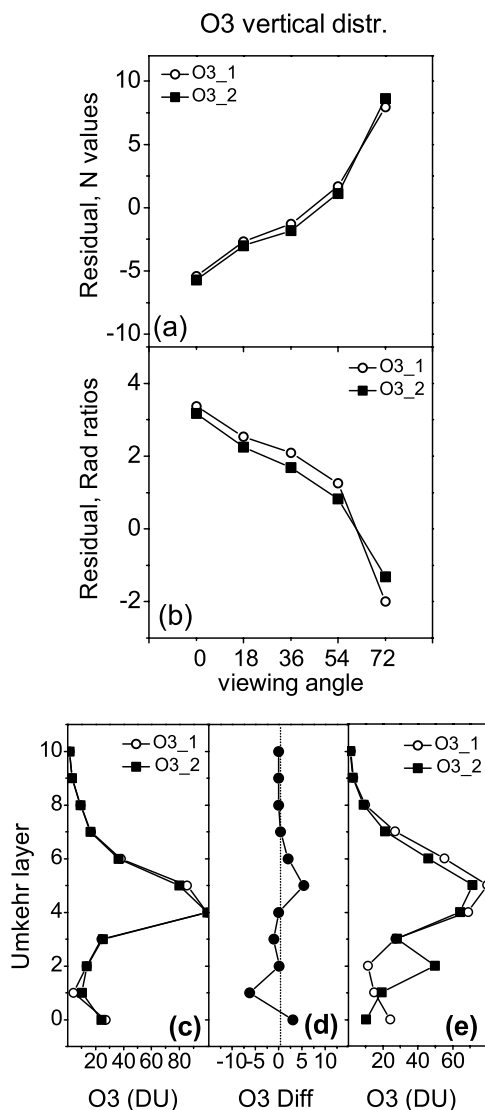


Figure 9. (a–d) Similar to Figure 8 but for the effect of O₃ vertical distribution on estimated aerosol correction. (e) The two different O₃ profiles that were used to estimate the two different aerosol corrections.

Brewer data, since the Brewer spectrometer also obtains sun and sky radiances near 340 nm that are less affected by O₃ absorption. Including these measurements in the retrieval would allow solving simultaneously for aerosol parameters and O₃ distribution for each retrieved O₃ profile.

4. Summary and Conclusions

[47] A new practical method is described for retrieving accurate stratospheric and tropospheric O₃ profiles from measured UV-B sky radiances in the presence of aerosols. The O₃ retrieval method is based on an optimal estimation technique that minimizes residuals between measured and calculated sky radiances constrained by measured total column O₃ amount and stabilized by using a climatological set of a priori O₃ profiles. Stratospheric O₃ profiles are obtained at large SZAs (>75°), when the averaging kernels show sensitivity to the stratospheric ozone. The retrieved

stratospheric profile shape is then used to constrain retrievals of tropospheric O₃ profiles at smaller SZAs, when the averaging kernels show increased sensitivity to the tropospheric ozone. The retrieval is performed under the assumption that the stratospheric profile shape remains constant throughout the day. The averaging kernels show that at least two to three ozone values can be retrieved in the troposphere for every Brewer spectral measurement (typically every 30 min) throughout a substantial portion of each day. The method was tested using both simulated and measured sky radiances.

[48] Measurements of sky radiances were made with a modified Brewer double spectrometer that eliminates instrumental polarization sensitivity. This is essential, since aerosols modify the polarization state of the atmosphere and the absolute values of measured sky radiances. Improperly corrected measured sky radiances in the presence of aerosols lead to a systematic angular dependence in the retrieved N value residuals and an incorrect O₃ profile retrieval.

[49] The results of this study suggest that it is critical to include the effects of aerosols in the retrieval algorithm. The O₃ retrieval was mostly sensitive to AOT, which can be estimated at a high accuracy (1-sigma error of 0.02) from nearly simultaneous Brewer direct-sun measurements. The best current method of obtaining an aerosol correction, as needed for reliable tropospheric O₃ profile retrievals, is based on colocated aerosol measurements (e.g., using the Brewer direct-sun AOT, AERONET-derived PSD, MPL measurements of aerosol vertical distribution, and UV-MFRSR-derived SSA). Sensitivity studies have shown that the total error due to uncertainties in aerosol model parameters (estimated as the square root of the sum of the squares of individual errors due to uncertainties in AOT, SSA, and PSD) is ± 2 DU in Umkehr layers 0 to 5 with no significant error at higher altitudes. Near the O₃ maximum (e.g., Umkehr layer 4), the profile accuracy is controlled by the retrieved total column O₃ (measured at an accuracy of 0.5%) and the large SZA retrievals of stratospheric ozone. Future work will be directed toward more extensive validation of the O₃ retrieval and additional comparisons between retrieved O₃ profiles, balloon ozonesondes and ozone lidar measurements. Ongoing efforts include extending this technique to longer wavelengths (e.g., Brewer sky radiances at 340 nm) for simultaneous retrieval of O₃ vertical distribution and aerosol parameters.

[50] **Acknowledgments.** Funds for this work were provided by NASA. We thank Richard McPeters, Pawan K. Bhartia, and three anonymous reviewers for their constructive comments. We would also like to acknowledge contributions from Dave Larko, Dave Flittner, Robert Spurr, Bojan Bojkov, Jacquelyn C. Witte, and Anne Thompson's SHADOZ ozonesonde program.

References

- Arola, A., S. Kazadzis, N. Krotkov, A. Bais, J. Herman, and K. Lakkala (2005), Assessment of TOMS UV bias due to the absorbing aerosols, *J. Geophys. Res.*, **110**, D23211, doi:10.1029/2005JD005913.
- Bais, A. F., A. Kazantzidis, S. Kazadzis, D. S. Balis, C. S. Zerefos, and C. Meteli (2005), Deriving an effective aerosol single scattering albedo from spectral surface UV irradiance measurements, *Atmos. Environ.*, **39**, 1093–1102.
- Bates, D. R. (1984), Rayleigh scattering by air, *Planet. Space Sci.*, **32**, 785–790.
- Browell, E., S. Ismail, and S. Shipley (1985), Ultraviolet DIAL measurements of O₃ profiles in regions of spatially inhomogeneous aerosols, *Appl. Opt.*, **24**(17), 2827–2836.

- Burrows, J. P., A. Richter, A. Dehn, B. Deters, S. Himmelmann, S. Voigt, and J. Orphal (1999), Atmospheric remote sensing reference data from GOME: Part 2, Temperature-dependent absorption cross sections of O₃ in the 231–794 nm range, *J. Quant. Spectrosc. Radiat. Transfer*, **61**, 509–517.
- Carvalho, F., and D. Henriques (2000), Use of Brewer ozone spectrophotometer for aerosol optical depth measurements on ultraviolet region, *Adv. Space Res.*, **25**, 997–1006.
- Cede, A., and J. R. Herman (2005), Measurements of O₃, SO₂, NO₂ and HCHO column amounts using a Brewer spectrometer, in *Ultraviolet Ground- and Space-Based Measurements, Models, And Effects V*, vol. 5886, *Proceedings of SPIE*, edited by G. Bernhard, J. R. Slusser, J. R. Herman, and W. Gao, pp. 7–15, Int. Soc. for Opt. Eng., San Diego, Calif.
- Cede, A., J. R. Herman, A. Richter, N. Krotkov, and J. Burrows (2006a), Measurements of nitrogen dioxide total column amounts using a Brewer double spectrometer in direct Sun mode, *J. Geophys. Res.*, **111**, D05304, doi:10.1029/2005JD006585.
- Cede, A., S. Kazadzis, M. Kowalewski, A. Bais, N. Kouremeti, M. Blumthaler, and J. R. Herman (2006b), Correction of direct irradiance measurements of Brewer spectrophotometers due to the effect of internal polarization, *Geophys. Res. Lett.*, **33**, L02806, doi:10.1029/2005GL024860.
- Cheymol, A., and H. De Backer (2003), Retrieval of the aerosol optical depth in the UV-B at Uccle from Brewer ozone measurements over a long time period 1984–2002, *J. Geophys. Res.*, **108**(D24), 4800, doi:10.1029/2003JD003758.
- Dave, J. V. (1964), Meaning of successive iteration of the auxiliary equation of radiative transfer, *Astrophys. J.*, **140**, 1292–1303.
- Diffey, B. L. (1991), Solar ultraviolet radiation effects on biological systems, *Phys. Med. Biol.*, **36**, 299–328.
- Dubovik, O., B. Holben, T. Eck, A. Smirnov, Y. J. Kaufman, M. D. King, D. Tanre, and I. Slutsker (2002), Variability of absorption and optical properties of key aerosol types observed in worldwide locations, *J. Atmos. Sci.*, **59**, 590–608.
- Fioletov, V. E., E. Griffiths, J. B. Kerr, D. I. Wardle, and O. Uchino (1998), Influence of volcanic sulfur dioxide on spectral UV irradiance as measured by Brewer spectrophotometers, *Geophys. Res. Lett.*, **25**, 1665–1668.
- Fishman, J., C. E. Watson, J. C. Larsen, and J. A. Logan (1990), Distribution of tropospheric ozone determined from satellite data, *J. Geophys. Res.*, **95**, 3599–3617.
- Gao, W., J. Slusser, J. Gibson, G. Scott, D. Bigelow, J. Kerr, and B. McArthur (2001), Direct-sun column ozone retrieval by the ultraviolet multifilter rotating shadow-band radiometer and comparison with those from Brewer and Dobson spectrophotometers, *Appl. Opt.*, **40**(19), 3149–3155.
- Groebner, J., R. Vergaz, V. E. Cachorro, D. V. Henriques, K. Lamb, A. Redondas, J. M. Vilaplana, and D. Rembges (2001), Intercomparison of aerosol optical depth measurements in the UV-B using Brewer spectrophotometers and a Li-Cor spectrophotometer, *Geophys. Res. Lett.*, **28**, 1691–1694.
- Guo, X., V. Natraj, D. R. Feldman, R. J. D. Spurr, R. Shia, S. P. Sander, and Y. Yung (2007), Retrieval of ozone profile from ground-based measurements with polarization: A synthetic study, *J. Quant. Spectrosc. Radiat. Transfer*, **103**, 175–192.
- Herman, B. M., T. R. Caudill, D. E. Flittner, K. J. Thome, and A. Ben-David (1995), A comparison of the Gauss-Seidel spherical polarized radiative transfer code with other radiative transfer codes, *Appl. Opt.*, **34**(21), 4563–4572.
- Holben, B. N., et al. (1998), AERONET - A federated instrument network and data archive for aerosol characterization, *Remote Sens. Environ.*, **66**, 1–16.
- Hoogen, R., V. V. Rozanov, K. Bramstedt, K. U. Eichmann, M. Weber, and J. P. Burrows (1999), O₃ profiles from GOME satellite data-I: Comparison with ozonesonde measurements, *Phys. Chem. Earth, Part C*, **24**(5), 447–452.
- Kazadzis, S., A. Bais, N. Kouremeti, E. Gerasopoulos, K. Garane, M. Blumthaler, B. Schallhart, and A. Cede (2005), Direct spectral measurements with a Brewer spectroradiometer: Absolute calibration and aerosol optical depth retrieval, *Appl. Opt.*, **44**(9), 1681–1690.
- Kerr, J. B., C. T. McElroy, and R. A. Olafson (1981), Measurements of ozone with the Brewer spectrophotometer, in *Proceedings of the Quadrennial Ozone Symposium*, edited by J. London, pp. 74–79, Natl. Cent. for Atmos. Res., Boulder, Colo.
- Kerr, J. B., C. T. McElroy, D. I. Wardle, R. A. Olafson, and W. F. J. Evans (1985), The automated Brewer spectrophotometer, in *Atmospheric Ozone: Proceedings of the Quadrennial Ozone Symposium*, edited by C. S. Zerefos and A. Ghazi, pp. 396–401, Springer, Hingham, Mass.
- Kerr, J. B., I. A. Asbridge, and W. F. J. Evans (1988), Intercomparison of total ozone measured by the Brewer and Dobson spectrophotometers at Toronto, *J. Geophys. Res.*, **93**, 11,129–11,140.
- Krotkov, N. A., P. K. Bhartia, J. R. Herman, J. Slusser, G. Scott, G. Janson, G. Labow, T. Eck, and B. Holben (2005a), Aerosol UV absorption experiment (2002 to 2004), 1. UV-MFRSR calibration and intercomparison with CIMEL sunphotometers, *Opt. Eng.*, **44**(4), 141004, doi:10.1117/1.1886818.
- Krotkov, N. A., P. K. Bhartia, J. R. Herman, J. Slusser, G. Scott, G. Labow, A. Vasilkov, T. Eck, O. Dubovik, and B. Holben (2005b), Aerosol UV absorption experiment (2002 to 2004), 2. Absorption optical thickness, refractive index, and single scattering albedo, *Opt. Eng.*, **44**(4), 041005, doi:10.1117/1.1886819.
- Krotkov, N. A., et al. (2007), Spectral measurements of aerosol absorption from UV to visible wavelengths, *EOS Trans. AGU*, **88**(23), Jt. Assem. Suppl., Abstract A51B-08.
- Liu, X., C. E. Sioris, K. Chance, T. P. Kurosu, M. J. Newchurch, R. V. Martin, and P. I. Palmer (2005), Mapping tropospheric ozone profiles from an airborne ultraviolet-visible spectrometer, *Appl. Opt.*, **44**(16), 3312–3319.
- Liu, X., K. Chance, C. E. Sioris, M. J. Newchurch, and T. P. Kurosu (2006), Tropospheric ozone profiles from a ground-based ultraviolet spectrometer: A new retrieval method, *Appl. Opt.*, **45**(10), 2352–2359.
- Liu, X., K. Chance, and T. P. Kurosu (2007), Improved ozone profile retrievals from GOME data with degradation correction in reflectance, *Atmos. Chem. Phys. Disc.*, **7**, 1575–1583.
- Mateer, C. L. (1965), On the information content of Umkehr observations, *J. Atmos. Sci.*, **22**, 370–381.
- McDermid, I. S., T. D. Walsh, A. Deslis, and M. L. White (1995), Optical-systems design for a stratospheric lidar system, *Appl. Opt.*, **34**(27), 6201–6210.
- McDermid, I. S., G. Beyerle, D. A. Haner, and T. Leblanc (2002), Redesign and improved performance of the tropospheric ozone lidar at the Jet Propulsion Laboratory Table Mountain Facility, *Appl. Opt.*, **41**(36), 7550–7555.
- McGee, T. J., M. R. Gross, U. N. Singh, J. J. Butler, and P. E. Kimvilakani (1995), Improved stratospheric ozone lidar, *Opt. Eng.*, **34**(5), 1421–1430.
- McPeters, R. D., G. J. Labow, and J. A. Logan (2007), Ozone climatological profiles for satellite retrieval algorithms, *J. Geophys. Res.*, **112**, D05308, doi:10.1029/2005JD006823.
- Palm, M., C. von Savigny, T. Warneke, V. Velasco, J. Notholt, K. Kunzi, J. Burrows, and O. Schrems (2005), Intercomparison of O₃ profiles observed by SCIAMACHY and ground based microwave instruments, *Atmos. Chem. Phys.*, **5**, 2091–2098.
- Petropavlovskikh, I., P. K. Bhartia, and J. DeLuisi (2005), New Umkehr ozone profile retrieval algorithm optimized for climatological studies, *Geophys. Res. Lett.*, **32**, L16808, doi:10.1029/2005GL023323.
- Rault, D. F. (2005), Ozone profile retrieval from Stratospheric Aerosol and Gas Experiment (SAGE III) limb scatter measurements, *J. Geophys. Res.*, **110**, D09309, doi:10.1029/2004JD004970.
- Rodgers, C. (2000), *Inverse Methods for Atmospheric Sounding: Theory and Practice*, World Sci., Hackensack, N. J.
- Rodgers, C., et al. (1998), Information content of ozone retrieval algorithms, in *Report of the International Ozone Trends Panel 1988, Global Ozone Research and Monitoring Project, Rep. 18*, chap. 3., World Meteorol. Organ., Geneva, Switzerland.
- Schoeberl, M. R., et al. (2006), Overview of the EOS Aura Mission, *IEEE Trans. Geosci. Remote Sens.*, **44**(5), 1066–1074, doi:10.1109/TGRS.2005.861950.
- Slusser, J. R., D. Kolinski, W. F. Mou, G. Koenig, J. H. Gibson, and D. S. Bigelow (1999), Comparison of column ozone retrievals from 3 different ground-based spectral measurements, *Appl. Opt.*, **38**(9), 1543–1551.
- Taubman, B. F., J. C. Hains, A. M. Thompson, L. T. Marufu, B. G. Doddridge, J. W. Stehr, C. A. Piety, and R. R. Dickerson (2006), Aircraft vertical profiles of trace gas and aerosol pollution over the mid-Atlantic United States: Statistics and meteorological cluster analysis, *J. Geophys. Res.*, **111**, D10S07, doi:10.1029/2005JD006196.
- Tevini, M. (Ed.) (1993), Effects of enhanced UV-B radiation on terrestrial plants, in *UV-B Radiation and Ozone Depletion*, pp. 125–154, A. F. Lewis, New York.
- Thompson, A. M., et al. (2003), Southern Hemisphere Additional Ozone-sondes (SHADOZ) 1998–2000 tropical ozone climatology 2. Tropospheric variability and the zonal wave-one, *J. Geophys. Res.*, **108**(D2), 8241, doi:10.1029/2002JD002241.
- Uthe, E., J. Livingston, and N. Nielsen (1992), Airborne lidar mapping of ozone concentrations during the Lake Michigan ozone study, *J. Air Waste Manage. Assoc.*, **42**, 1313–1318.
- Ziemke, J. R., and S. Chandra (1999), Seasonal and interannual variabilities in tropical tropospheric ozone, *J. Geophys. Res.*, **104**, 21,425–21,442.
- Ziemke, J. R., S. Chandra, B. N. Duncan, L. Froidevaux, P. K. Bhartia, P. F. Levelt, and J. W. Waters (2006), Tropospheric ozone determined from

Aura OMI and MLS: Evaluation of measurements and comparison with the Global Modeling Initiative's Chemical Transport Model, *J. Geophys. Res.*, *111*, D19303, doi:10.1029/2006JD007089.

A. Cede and M. Tzortziou, Earth System Science Interdisciplinary Center, University of Maryland, College Park, MD 20742-2465, USA. (maria.a.tzortziou@nasa.gov)

J. R. Herman, NASA Goddard Space Flight Center, Greenbelt, MD 20771, USA.

N. A. Krotkov, Goddard Earth Science and Technology Center, University of Maryland, Baltimore County, Baltimore, MD 21250, USA.

A. Vasilkov, Science Systems and Applications Incorporated, Lanham, MD 20706, USA.